THE UNIVERSITY of EDINBURGH

Edinburgh Research Explorer

Laser detection of spin-polarized hydrogen from HCl and HBr photodissociation: Comparison of H- and halogen-atom polarizations

Citation for published version:
Sofikitis, D, Rubio-Lago, L, Bougas, L, Alexander, AJ & Rakitzis, TP 2008, 'Laser detection of spin-polarized hydrogen from HCl and HBr photodissociation: Comparison of H- and halogen-atom polarizations' The Journal of Chemical Physics, vol. 129, no. 14, 144302 . DOI: 10.1063/1.2989803

Digital Object Identifier (DOI):
10.1063/1.2989803

Link:
Link to publication record in Edinburgh Research Explorer

Document Version:
Publisher's PDF, also known as Version of record

Published In:
The Journal of Chemical Physics

OPEN ACCESS

Laser detection of spin-polarized hydrogen from HCl and HBr photodissociation: Comparison of H- and halogen-atom polarizations

Dimitris Sofikitis, Luis Rubio-Lago, Lykourgos Bougas, Andrew J. Alexander, and T. Peter Rakitzis

---

Additional information on J. Chem. Phys.

Laser detection of spin-polarized hydrogen from HCl and HBr photodissociation: Comparison of H- and halogen-atom polarizations

Dimitris Sofikitis,[1,2] Luis Rubio-Lago,[2] Lykourgos Bougas,[1,2] Andrew J. Alexander,[3] and T. Peter Rakitzis[1,2,a)]

[1]*Department of Physics, University of Crete, 71003 Heraklion-Crete, Greece*
[2]*Institute of Electronic Structure and Laser, Foundation for Research and Technology-Hellas, 71110 Heraklion-Crete, Greece*
[3]*School of Chemistry, University of Edinburgh, West Mains Road, Edinburgh EH9 3JJ, United Kingdom*

Thermal HCl and HBr molecules were photodissociated using circularly polarized 193 nm light, and the speed-dependent spin polarization of the H-atom photofragments was measured using polarized fluorescence at 121.6 nm. Both polarization components, described by the $a_0^1(\perp)$ and $\mathrm{Re}[a_1^1(\parallel, \perp)]$ parameters which arise from incoherent and coherent dissociation mechanisms, are measured. The values of the $a_0^1(\perp)$ parameter, for both HCl and HBr photodissociation, are within experimental error of the predictions of both *ab initio* calculations and of previous measurements of the polarization of the halide cofragments. The experimental and *ab initio* theoretical values of the $\mathrm{Re}[a_1^1(\parallel, \perp)]$ parameter show some disagreement, suggesting that further theoretical investigations are required. Overall, good agreement occurs despite the fact that the current experiments photodissociate molecules at 295 K, whereas previous measurements were conducted at rotational temperatures of about 15 K. © *2008 American Institute of Physics*. [DOI: 10.1063/1.2989803]

I. INTRODUCTION

The measurement of photofragment angular momentum polarization is an extremely sensitive probe of photodissociation dynamics and offers a powerful method for measuring nonadiabatic-transfer probabilities and asymptotic phase shifts between wavefunctions of dissociative states.[1–7] Such measurements are becoming routine, especially since the pioneering work of Siebbeles *et al.*;[7] however, most of these measurements have been limited to a handful of atoms which have convenient laser-detection schemes, such as Cl,[8–13] Br,[9,11,13] O,[14–20] and S.[21–26] Conspicuously absent in photofragment polarization studies has been the ground state of the simplest atom, hydrogen, although mechanisms for the polarization of H atoms from hydrogen halide photodissociation have been discussed for some time.[10,27,28] In contrast, the fluorescence of excited H-atom states from the photodissociation of H_2 have been studied extensively.[29–34] The main reason for the lack of studies on ground-state H-atom photofragments has been that spin-sensitive detection of H atoms has—until now—been achieved only by resolving the fine structure of the $2p \leftarrow 1s$ transition;[35–37] this requires that the Doppler spread of the H atoms be very small, which will occur either in collimated atomic beams or from samples having a translational temperature of less than about 80 K. This constraint does not allow H-atom spin polarization to be detected without some stringent form of velocity selection; one example is the detection of H and D atoms from HCl and DCl photodissociation, by Koplitz and co-workers,[37–40] using velocity-aligned Doppler spectroscopy (VADS), which allows selective excitation of the fine structure of H-atom photofragments traveling parallel to the probe beam. This spatial velocity selection is achieved by detecting only the H atoms that have traveled about 0.5 m from the photolysis region to the probe, after a long time delay. However, this method is highly specialized and is not applicable to most sources of spin-polarized H atoms. For the experimental systems chosen by Koplitz and co-workers polarizations of zero, within experimental error, were measured.

Recently, the speed-dependent spin polarization of H atoms was measured without requiring hyperfine resolution, using polarized fluorescence, for the photodissociation of HBr.[41] Hyperfine resolution is unnecessary, provided that (1) the probe laser light is circularly polarized, (2) the fluorescence is collected perpendicular to the probe propagation direction, and (3) the fluorescence is first passed via a linear polarizer (which passes light polarized parallel to the probe propagation direction).[42] Using these polarization constraints, the spin polarization of the H atoms is measured averaged over the bandwidth of the probe light. Hence, the experiment does not require resolution of the fine structure of the H-atom transition; the bandwidth of the probe light merely determines the Doppler (velocity) resolution of the experiment. For the photodissociation of HBr with circularly polarized 193 nm light, the electronic spin polarization of the nascent H atoms (before hyperfine spin polarization) was found to be at least 60%.[41] The aims of this paper are to give a detailed description of the experimental procedures and checks necessary for the detection of the spin polarization of H atoms and to present results for the photodissociation of HCl at 193 nm, comparing them to the previously published results of the photodissociation of HBr,[41] with *ab initio*

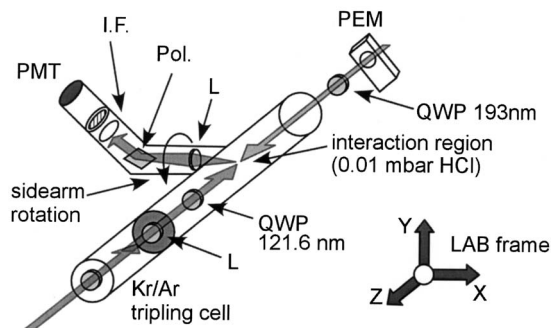a)Electronic mail: ptr@iesl.forth.gr.

FIG. 1. (a) Schematic of the experimental setup (L, MgF$_2$ lens; IF, 121.6 nm interference filter; Pol., 121.6 nm Brewster polarizer; PMT, photomultiplier tube; PEM, photoelastic modulator; QWP, and quarter-wave plate). The $+Z^{lab}$ axis is defined by the direction of the left circularly polarized (LCP) 193 nm light pulse that dissociates HBr or HCl to produce SPH. The counterpropagating probe laser excites the SPH from the 1s to the 2p state, and the resulting fluorescence is first polarized and collected by a photomultiplier tube, collecting fluorescence perpendicular to Z^{lab}, but linearly polarized parallel to Z^{lab}. The complete rotation of the side arm of the vacuum chamber, including the polarizer and the detector, can be achieved so as to collect fluorescence that is polarized parallel to Y^{lab}.

theory[43,44] and with past measurements of the polarization of the halogen cofragments from the photodissociation of HCl and HBr.[10,13]

II. EXPERIMENTAL

A schematic of the experimental setup is shown in Fig. 1. Neat HBr or HCl is leaked into a vacuum chamber, and the pressure of the room-temperature gas is measured with a capacitance manometer (typically about 10 μbars were used). The photolysis and probe laser beams counterpropagate through the chamber. The photolysis laser beam, at 193 nm, is generated by an ArF excimer laser (PSX-501, Neweks, Estonia), which is first linearly polarized by reflecting from a thin-film polarizer (Laseroptik, Germany), then circularly polarized using a zero-order quarter-wave plate, and finally is focused at the interaction region (focal length f=50 cm); the laser output of the 193 nm light was about 5 mJ pulse^{-1}. A photoelastic modulator (PEM-80, Hinds Instruments) is placed before the quarter-wave plate. Synchronization to the stress cycle of the PEM allowed the linear polarization of the light to be alternated between vertical and horizontal; after passing through the quarter-wave plate, the photolysis laser polarization alternates between right and left circular polarization states on a shot-to-shot basis. Both photolysis and probe lasers were operated at 10 Hz.

The probe laser beam, at 121.6 nm, is generated by frequency-tripling 364.7 nm light (from the output of an excimer-pumped dye laser system) in a krypton/argon gas mixture, and the beam is then focused into the vacuum chamber with a magnesium fluoride (MgF$_2$) lens. The 121.6 nm light generated is linearly polarized and is made circularly polarized by passing it, under vacuum, through a MgF$_2$ variable wave plate (Alphalas, Germany); the tilt angle (about an axis which was set at 45° to the polarization axis of the 364.7 nm light and hence also to the polarization axis of the 121.6 nm light) is varied until the 121.6 nm light is circularly polarized. The experimental check for verifying the

circular polarization of the 121.6 nm probe light was detection of the H-atom fluorescence intensity as the 364.7 nm light was alternated between horizontal and vertical linear polarization states. When the phase shift of the variable wave plate is 0, the polarization of the 121.6 nm light also alternates linearly between horizontal and vertical; when the phase shift is π (half-wave retardation) it alternates between vertical and horizontal; and when the phase shift is $\pi/2$ (quarter-wave retardation) it alternates between right and left circular polarization states. As discussed below, the fluorescence intensity ratio, ($I_\parallel/I_\perp$), between the 121.6 nm fluorescence polarization axis being parallel ($I_\parallel$) and perpendicular ($I_\perp$) to the polarization direction of the excitation light is 5:2. Initially, with respect to the 364.7 nm light polarization axis (which is parallel to the 121.6 nm polarization axis), a ratio of about 5:2 is measured. When the variable wave plate introduces a phase shift of π, and the vertical and horizontal polarization states of the 121.6 nm light are exchanged (using a half wave-plate), then the polarization ratio with respect to the 364.7 nm light polarization axes is inverted to be 2:5. The intermediate point, where the ratio is 1:1, is where the 121.6 nm light is circularly polarized. However, the signal-to-noise ratio on this fluorescence signal was about 10:1 so that the degree of the circular polarization of the 121.6 nm light could only be determined to be in excess of about 90%. Other methods for generating 121.6 nm exist (not currently available to us), such as four-wave mixing, which can produce more light intensity, and where the polarization of the 121.6 nm light can be controlled more directly by varying the polarization of visible light, obviating the need for the manipulation of polarization optics in vacuum.

The 121.6 nm fluorescence was collected perpendicular to the laser propagation direction. It was collected and collimated with a MgF$_2$ lens (f=12 cm). The fluorescence was linearly polarized parallel to the laser propagation direction by reflecting it from a MgF$_2$ plate at Brewster's angle (about 58.5° for 121 nm light) and was passed through a 121.6 nm interference filter with a 10 nm bandwidth (Acton Research Corp., Acton, MA, USA), and finally the fluorescence was detected with a photomultiplier tube (9403B, Electron Tubes, UK). All collection optics and the variable waveplate were held under vacuum (all in the same chamber) and were routinely subjected to pressures of HBr or HCl of up to 1 mbar, without significant adverse effects (cleaning of the optics, especially following use with HBr, was required every few days.).

H atoms were detected via the $2p \leftarrow 1s$ transition at about 121.6 nm. For experimental checks of the detection scheme, H atoms were generated from collisions of background contaminants, such as pump oil, with a nude ion gauge to produce H atoms which, upon thermalization in the chamber, possessed translational temperatures of about 300 K. For these H atoms, the Doppler spread was small enough that some evidence of fine-structure resolution was observed (though mostly unresolved; see below). The two transitions involved were the $^2P_{1/2} \leftarrow {}^2S_{1/2}$ and $^2P_{3/2} \leftarrow {}^2S_{1/2}$, which, with linearly polarized light, are excited with probability 1:2. The $^2P_{1/2}$ state fluoresces isotropically since J=1/2; in contrast, the $^2P_{3/2}$ state, populated only in the

$m = \pm 1/2$ states from $^2P_{3/2} \leftarrow {}^2S_{1/2}$ excitation with linearly polarized light, fluoresces anisotropically, which can be described by the fluorescence polarization anisotropy R:[45]

$$R = \frac{I_\parallel - I_\perp}{I_\parallel + 2I_\perp},\tag{1}$$

where $I_\parallel$ and $I_\perp$ are defined above. For a $\Delta J = +1$ transition, as for the $^2P_{3/2} \leftarrow {}^2S_{1/2}$ transition, the polarization anisotropy is given by[45]

$$R = \frac{(J_i + 2)(2J_i + 5)}{10(J_i + 1)(2J_i + 1)},\tag{2}$$

where J_i is the angular momentum of the ground state. For $J_i = 1/2$, $R = 1/2$, which yields, from Eq. (1), a fluorescence polarization ratio $(I_\parallel/I_\perp) = 4$. Therefore, for the $^2P_{1/2} \leftarrow {}^2S_{1/2}$ and $^2P_{3/2} \leftarrow {}^2S_{1/2}$ transitions, the fluorescence polarization ratios $(I_\parallel/I_\perp)$ are 1 and 4, respectively. We note that the $2p$ hyperfine depolarization times are more than 15 times longer than the $2p$ fluorescence lifetime of 1.1 ns so that hyperfine structure can be ignored in the calculation of the $(I_\parallel/I_\perp)$ polarization ratio. Averaging the two transitions (and noting that the fluorescence intensity ratio over all space between the two transitions is 1:2, equal to the excitation probability ratio), the $(I_\parallel/I_\perp)$ ratio for the unresolved $2p \leftarrow 1s$ transition is found to be 2.5 ideally. The calculation of this ratio assumes that all the optics behave ideally and that the fluorescence of the H atoms is unperturbed by external factors such as fields or collisions. Therefore, the measurement of these polarization ratios serves as an important experimental test of the detection scheme.

The polarization ratio $(I_\parallel/I_\perp)$ can be used to describe all four polarization ratios that can be realized in our experimental geometry (see Fig. 1; note that the detection system can be rotated so that fluorescence linearly polarized along either Z^{lab} or Y^{lab} can be detected). These are described by the signal intensities I_{FG}, where F denotes the axis of the excitation polarization and G denotes the axis of the fluorescence polarization. For example, I_{XY} denotes the signal intensity with the excitation polarization axis parallel to X and the fluorescence polarization axis parallel to Y. We can then deduce the following polarization ratios:

$$\frac{I_{YY}}{I_{YZ}} = 2.5,\tag{3a}$$

$$\frac{I_{XY}}{I_{XZ}} = 1,\tag{3b}$$

$$\frac{I_{YY}}{I_{XY}} = 2.5,\tag{3c}$$

$$\frac{I_{YZ}}{I_{XZ}} = 1.\tag{3d}$$

In addition, detection without the use of a polarizer (the label O is used here to denote the lack of polarization selection for the detection step) gives
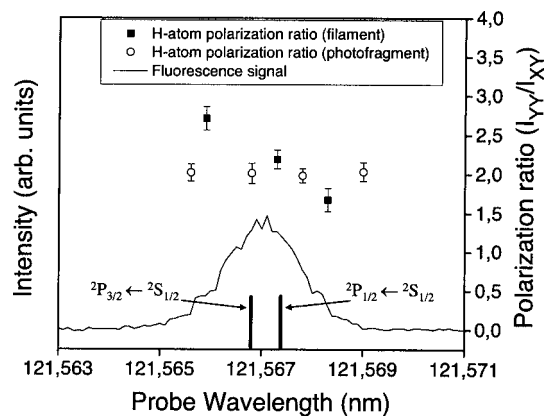

FIG. 2. Scan of the 121.6 nm probe laser over the $2p \leftarrow 1s$ transition of H atoms produced from a nude ion gauge and with a translational temperature of about 300 K. No fine-structure resolution is visible. Measurement of the polarization ratio I_{YY}/I_{XY} at three different probe wavelengths within the profile (solid squares) shows that the ratio I_{YY}/I_{XY} varies strongly with probe wavelength, demonstrating some degree of fine-structure resolution (see text). In contrast, measurements from H-atom photofragments from the photodissociation of HCl at about 0.2 mbar, with speeds of about 19 km s^{-1} (open circles), show that the ratio I_{YY}/I_{XY} does not vary significantly over a larger wavelength range and thus does not show any fine-structure resolution.

$$\frac{I_{YO}}{I_{XO}} = \frac{1}{2}\left[\frac{I_{YY}}{I_{XY}} + \frac{I_{YZ}}{I_{XZ}}\right] = \frac{1}{2}\left[\frac{I_{YY}}{I_{XY}} + 1\right].\tag{4}$$

Only the ratio (I_{YZ}/I_{XZ}) has been substituted with its value of 1 because depolarization mechanisms cannot alter this value; in contrast, depolarization mechanisms, such as depolarizing collisions with the excited H atoms, can cause the fluorescence ratios in Eqs. (3a) and (3c) to be reduced. Equation (4), therefore, describes the relationship between unpolarized fluorescence detection ratio (I_{YO}/I_{XO}) and the ratio (I_{YY}/I_{XY}); as (I_{YY}/I_{XY}) ranges from the maximum value of 2.5 (no depolarization) down to 1 (complete depolarization), so (I_{YO}/I_{XO}) ranges from 1.75 to 1.

Equations (3a)–(3d) are used to check the performance of detection system. For our experimental setup, rotation of the excitation polarization between the X and Y axes can be achieved robustly with a $\lambda/2$ plate. In contrast, rotation of the polarizer in the detection system from the Y and Z axis involves a physical rotation of the side arm of the vacuum chamber, which may alter the collection efficiency at the detector. Any such variation, in our case, is observed to be small, as the ratio (I_{XY}/I_{XZ}) is measured to be 1 within our experimental error. In Fig. 2, we show a scan of the probe laser over the $2p \leftarrow 1s$ transition, using light linearly polarized along the Y and X axes and detecting fluorescence linearly polarized along the Y axis; the probed H atoms are produced by a nude ion gauge and are at a temperature of about 300 K. Even though the signal appears to show only one peak, with no apparent resolution of the $^2P_{1/2} \leftarrow {}^2S_{1/2}$ and $^2P_{3/2} \leftarrow {}^2S_{1/2}$ transitions, measurements of the (I_{YY}/I_{XY}) polarization ratio across the profile show values that differ from the predicted integrated average ratio of 2.5. These variations show some sensitivity to the resolution of the $^2P_{1/2} \leftarrow {}^2S_{1/2}$ and $^2P_{3/2} \leftarrow {}^2S_{1/2}$ transitions as their (I_{YY}/I_{XY}) polarization ratios are 1 and 4, respectively. This shows that the H atoms
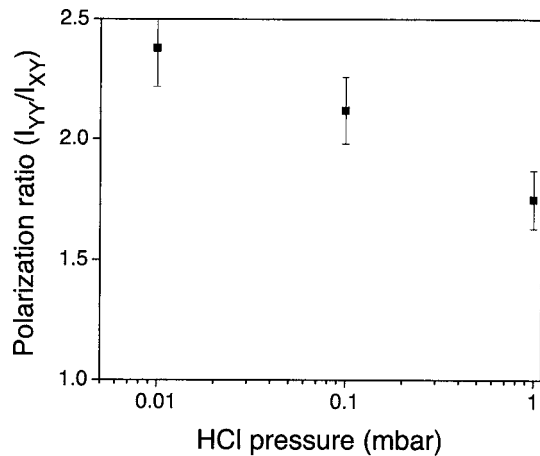
FIG. 3. Measurement of the polarization ratio I_{YY}/I_{XY} as a function of HCl pressure. At higher pressures, the ratio I_{YY}/I_{XY} decreases from the ideal value of 2.5, indicating depolarization from collisions.
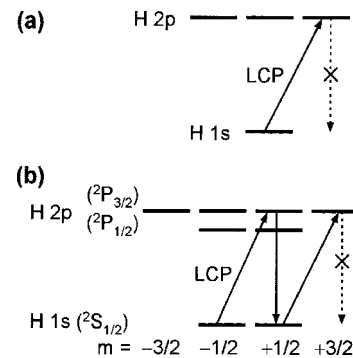

FIG. 4. (a) Energy-level detection scheme, showing that no signal is detected in the limit of no spin-orbit coupling. (b) Similar to (a), but with spin-orbit coupling, showing that only the $m=-1/2$ spin state is detected using LCP 121.6 nm probe light.

from the nude ion gauge are not ideal for the polarization calibration of the detection system as integration over the Doppler peak is necessary (which increases acquisition times and sensitivity to experimental instabilities) and the density of the H atoms cannot be measured easily or controlled quantitatively. Therefore, all polarization tests were performed on H atoms from the photodissociation of HCl at 193 nm; these H atoms have a very large Doppler spread so that there is no partial resolution of the fine-structure transitions, and the density of the H atoms can be varied quantitatively by varying the pressure of the HCl. In Fig. 2, measurements of fluorescence ratio (I_{YY}/I_{XY}) from H atoms from the photodissociation of HCl at a pressure of 0.2 mbar show no significant variation over a wavelength range larger than the fine-structure splitting.

In Fig. 3, we show the polarization ratio (I_{YY}/I_{XY}) measured from H atoms from the photodissociation of HCl as a function of HCl pressure. We see that the ratio increases and tends toward the ideal value of 2.5 as the pressure is decreased. The lowest pressure we were able to work at confidently was about 0.01 mbar, which is the pressure at which all subsequent experiments were conducted. A discussion of the detection of the spin polarization follows, to understand how degradation in the measured (I_{YY}/I_{XY}) ratio affects the sensitivity of the detection of the spin polarization.

The H atoms are excited from the $1s\ ^2S_{1/2}$ to the $2p\ ^2P_J$ states using circularly polarized 121.6 nm light. The 121.6 nm fluorescence of the excited atoms is detected perpendicular to the propagation of the excitation laser, and a polarizer is used to detect only fluorescence that is linearly polarized along the Z axis (see Fig. 1), which ensures that the polarization components of the transitions that are observed are those that correspond to $\Delta m=0$, irrespective of the original polarization of fluorescence (we note that the polarization components of the transitions that corresponded to $m=\pm 1$ are rejected by the polarizer). The geometry of the experiment has been chosen so that angular momentum selection rules constrain the excitation and fluorescence processes to be allowed for only one of the spin states so that the H-atom spin polarization can be determined along the Z axis. The

success of the detection scheme relies on the coupling of the electron's spin to its orbital motion. If the H atoms were to fluoresce very rapidly, on a subpicosecond timescale where spin-orbit coupling can be ignored, our detector would see no fluorescence since, according to selection rules for linearly polarized fluorescence emission, $\Delta m=0$ [see Fig. 4(a)]. In contrast, for the ~ 1 ns fluorescence lifetime of the $2p$ state, we see that only atoms that originate from the $1s\ (m=-1/2)$ "spin-down" state, and that are excited to either of the $2p\ ^2P_J\ (m=+1/2)$ states, can subsequently fluoresce linearly polarized photons back to $1s\ (m=+1/2)$: no fluorescence can be detected from atoms that originate in the $1s\ (m=+1/2)$ "spin-up" state for this particular experimental geometry [see Fig. 4(b)]. The reverse applies for excitation by right circularly polarized light (with $\Delta m=-1$), whereby only the spin-up state can be detected. Thus, this detection scheme allows complete spin-state detection selectivity for spin-polarized hydrogen (SPH) in the ground state, assuming that all the optics and the H-atom fluorescence process behave ideally. In particular, if the extinction ratio of the 121.6 nm polarizer is poor, or if collisions with the excited H-atom cause the fluorescence spatial distribution to become depolarized, then the detection sensitivity will be reduced. This reduction can be described by the factor Q in the polarization detection expression[46]

$$I_{LL(RL)} = \left(\frac{I_0}{2}\right)\left[1 - \frac{\beta}{2}P_2(\cos\theta) \pm s_1 G_{av}^{(1)} Q\right.$$
$$\times \left\{\left(1 - \frac{\beta}{2}\right)a_0^1(\perp)\cos^2\theta\right.$$
$$\left.\left. - \frac{1}{\sqrt{2}}\mathrm{Re}[a_1^1(\|,\perp)]\sin^2\theta\right\}\right], \qquad (5)$$

where $\cos\theta$ is the normalized Doppler shift of the SPH atoms given by the velocity projection $v_z/|v|$ and ranges from -1 to $+1$. The parameter β describes the spatial distribution of the SPH atom velocities from the photodissociation of HCl or HBr. The $a_0^1(\perp)$ and $\mathrm{Re}[a_1^1(\|,\perp)]$ parameters describe the recoil-angle-dependent spin polarization of the H atoms. The hyperfine depolarization factor $G_{av}^{(1)}$ describes the time-averaged reduction of the spin polarization by the nuclear spin and is given by $G_{av}^{(1)}=1/2$. The detection sensi-
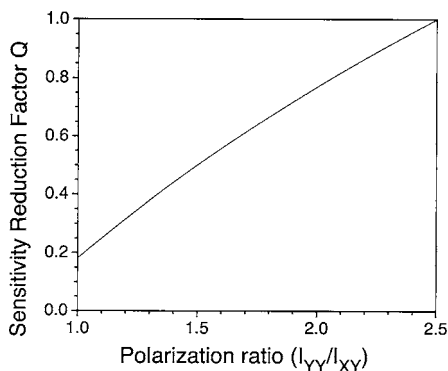
FIG. 5. The dependence of the sensitivity reduction factor Q on the polarization ratio I_{YY}/I_{XY}, from Eq. (6), showing that the reduction in sensitivity in the detection of the spin polarization of H atoms is small provided the ratio I_{YY}/I_{XY} is close to a maximal value of 2.5 (see Fig. 3).

FIG. 6. Adiabatic electronic potential energy curves of HCl, showing the five states that are relevant to the present study: $X(^3\Sigma_0^+)$, $A(^1\Pi_1)$, $a(^3\Pi_1)$, $a(^3\Pi_0^+)$, and $t(^3\Sigma_1)$. The potential energy curves for HBr are similar (see Fig. 1 of Ref. 43).

tivity s_1 describes the ideal spin-polarization detection sensitivity for this particular detection scheme and is given by $s_1 = \sqrt{3}$. The detection sensitivity of the $a_0^1(\perp)$ and $\mathrm{Re}[a_1^1(\|, \perp)]$ parameters depends on the relative helicity of the photolysis and probe lasers. The profiles are named according to the polarization state of the photolysis and probe laser beams; for example, I_{RL} indicates that the photolysis laser beam is right (R) circularly polarized and the probe laser beam is (L) circularly polarized. For the case where both laser beams were left circularly polarized (I_{LL}), the upper ($+$) sign is used before s_1. For the case of when the photolysis laser was right circularly polarized and the probe left circularly polarized (I_{RL}), the lower ($-$) sign is used before s_1 (the convention for the helicity of light used here is described elsewhere).[47] Finally, Q is the reduction in the spin-polarization detection sensitivity due to experimental factors such as depolarizing collisions. We calculate that the dependence of Q, on the fluorescence ratio (I_{YY}/I_{XY}), is given by

$$Q = \frac{2[4(I_{YY}/I_{XY}) - 3]}{[2(I_{YY}/I_{XY}) + 9]}. \tag{6}$$

For the maximal value of $(I_{YY}/I_{XY}) = 2.5$, there is no sensitivity reduction and $Q = 1$. If there is either maximal depolarization of the fluorescent light such that the fluorescence is unpolarized or if the fluorescence is detected with no polarization selectivity, then $(I_{YY}/I_{XY}) = 1$ and $Q = 2/11$. We note that Q is not zero in this case because this degree of spin-polarization sensitivity is achieved in the excitation step, and not in the detection step. In Fig. 5 we show the dependence of Q on the ratio (I_{YY}/I_{XY}) and see that at the lowest pressure of 0.01 mbar, where our experiments were conducted, with $(I_{YY}/I_{XY}) = 2.4 \pm 0.1$, the reduction in spin-polarization sensitivity is only about 5%, whereas at higher pressures the reduction increases. Since we operated with (I_{YY}/I_{XY}) values within error of the maximal value of 2.5 and could not conclusively determine that any reduction was actually present, we did not correct our measured values of H-atom spin polarization by 5% but included this uncertainty (small compared to our experimental error) in the upper bound of our error bars. Another group has performed experiments detecting the 121.6 nm fluorescence of aligned H
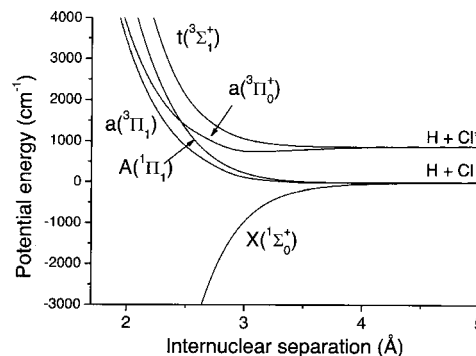
atoms in the $2p$ state from the photodissociation of H_2.[33] In these experiments, some depolarization of the H atoms was observed from collisions with H_2 at pressures of about 1 mbar, yielding a depolarization cross section of about 10^{-14} cm^2, and their results were corrected for this effect. We have also observed significant depolarization at HCl pressures of 1 mbar, but find that depolarization can be neglected at HCl pressures of around 0.01 mbar.

We note that without a polarizer in the detection step, the spin-polarization sensitivity is reduced by a factor of 2/11. We decided to use Brewster-angle reflection as a method of polarizing the 121.6 nm fluorescence because the extinction ratio was at least 20:1 (this measurement was limited by our signal-to-noise ratio), which is better than other polarizers used in the vacuum ultraviolet,[48] and the transmission is comparable to these other polarizers. Rotation of our polarizer involved the complete rotation of the side arm of the vacuum chamber, including the Brewster plate and the detector (see Fig. 1).

III. RESULTS AND DISCUSSION

Details of the HCl and HBr photodissociation at 193 nm have been published in the previous experimental and theoretical studies of the cofragment halogen-atom polarization.[10,13,43,44] To set the stage for discussion of the H-atom results, we make a brief review of the electronic states involved, as shown in Fig. 6. We will discuss primarily the case of HCl, but similar conclusions apply for HBr. There are five adiabatic electronic states, three that correlate to ground-state Cl($^2P_{3/2}$) and two that correlate to excited-state Cl*($^2P_{1/2}$). The long-range correlations to specific $|J, m\rangle$ states are summarized in Table I, and for brevity we shall refer to these states by $n\Omega$ as $X0$, $A1$, $a1$, $a0$, and $t1$. Excitation occurs mostly to the $A1$ state, with some excitation to $a0$. Previously published experimental measurements and *ab initio* calculations of the polarization parameters $a_0^1(\perp)$ and $\mathrm{Re}[a_1^1(\|, \perp)]$ of the halogen atoms are summarized in Table II. The measurements of the halogen-atom branching ratios, spatial distributions of the halogen atoms (described by the parameter β), and the polarization of the halogen atoms [in particular, the parameter $a_0^1(\perp)$] are together sufficient to determine the branching fractions into each of the five product

TABLE I. Electronic states involved in the 193 nm photodissociation of HCl and HBr. Y represents the halogen atom (Cl or Br). The product branching into ground and excited halogen atoms has been measured to be 0.59 (Cl) and 0.41 (Cl*) for HCl and 0.86 (Br) and 0.14 (Br*) for HBr. The corresponding spatial distributions of halogen atoms are described by $\beta=-0.97$ (Cl), $\beta=-0.87$ (Cl*), $\beta=-0.88$ (Br), and $\beta=-0.21$ (Br*). The orientation for ground-state atoms was reported to be $a_0^1(\perp)=0.39\pm0.08$ for Cl and $a_0^1(\perp)=0.3\pm0.03$ for Br (2σ error bars). In combination, these measurements are sufficient to determine the experimental branching into the five product electronic states, as given in the last two columns of the table for HCl and HBr.

Product channel	Electronic state	Designation	Product atom correlation $|J_H m_H; J_Y m_Y\rangle$	Experimental branching fractions HCl	Experimental branching fractions HBr
$H(^2P)+Y(^2P_{3/2})$	$X(^3\Sigma_0^+)$	$X0$	$\frac{1}{\sqrt{2}}\left[\left|\frac{1}{2}\frac{1}{2};\frac{3}{2}-\frac{1}{2}\right\rangle-\left|\frac{1}{2}-\frac{1}{2};\frac{1}{2}\frac{1}{2}\right\rangle\right]$	0.006	0.034
	$A(^1\Pi_1)$	$A1$	$\left|\frac{1}{2}-\frac{1}{2};\frac{3}{2}\frac{3}{2}\right\rangle$	0.149	0.067
	$a(^3\Pi_1)$	$a1$	$\left|\frac{1}{2}\frac{1}{2};\frac{3}{2}\frac{1}{2}\right\rangle$	0.435	0.759
$H(^2P)+Y^*(^2P_{1/2})$	$a(^3\Pi_0^+)$	$a0$	$\frac{1}{\sqrt{2}}\left[\left|\frac{1}{2}\frac{1}{2};\frac{1}{2}-\frac{1}{2}\right\rangle+\left|\frac{1}{2}-\frac{1}{2};\frac{1}{2}\frac{1}{2}\right\rangle\right]$	0.018	0.037
	$t(^3\Sigma_1)$	$t1$	$\left|\frac{1}{2}\frac{1}{2};\frac{1}{2}\frac{1}{2}\right\rangle$	0.392	0.103

electronic states, as described in the right-hand columns of Table I. To obtain the branching fractions we have assumed that only $\Delta\Omega=0$ nonadiabatic transitions occur. It is clear that a substantial amount of nonadiabatic interaction occurs, as has been discussed in detail elsewhere.

In Fig. 7(a) we show the I_{LL} and I_{RL} signal profiles of SPH from HCl photodissociation at 193 nm. Sums and differences of these profiles are taken [shown in Fig. 7(c)], which produce, respectively, signals that are independent of H-atom spin polarization, and proportional to H-atom spin polarization, from Eq. (5):

$$I_{LL}+I_{RL}=I_0[1-\beta(3\cos^2\theta-1)/4], \tag{7a}$$

$$I_{LL}-I_{RL}=I_0 s_1 G_{av}^{(1)}\left[\left(1-\frac{\beta}{2}\right)a_0^1(\perp)\cos^2\theta\right.$$
$$\left.-\frac{1}{\sqrt{2}}\operatorname{Re}[a_1^1(\parallel,\perp)]\sin^2\theta\right]. \tag{7b}$$

The data are fitted using Eqs. (7a) and (7b), similar to the case of the photodissociation of HBr which has been presented elsewhere.[41] As with HBr, the H-atom speeds are tightly peaked, with a 2.8% spread about 19.1 km s^{-1}; for HCl the spatial distribution is described by

$\beta=-0.93\pm0.06(2\sigma)$ and for HBr by $\beta=-0.79\pm0.10(2\sigma)$. The values of $a_0^1(\perp)$ and $\operatorname{Re}[a_1^1(\parallel,\perp)]$ resulting from the fits for both HCl and HBr photodissociation are plotted in Fig. 8, along with quantum mechanical *ab initio*-calculated values and predictions from previous measurements of the halogen-atom cofragments. The values are also summarized in Table III.

To infer the expected value of $a_0^1(\perp)$ from the halogen-atom measurements is relatively straightforward by conservation of angular momentum. The branching fractions into each of the five electronic states are given in Table I, and for each state we know the expected $|J_H, m_H\rangle$ state of the H atom. For $m_H=\pm1/2$ we have $a_0^1(\perp)=\pm1/\sqrt{3}$, respectively. The expected $a_0^1(\perp)$ for each state of the molecule may be weighted according to the branching fractions. We find that states where $\Omega=0$ contribute $a_0^1(\perp)=0$ to the weighted sum. The present experimental $a_0^1(\perp)$ parameters are found to be very close (within error) to both predictions of *ab initio* theory and predictions inferred from past experiments on the halogen cofragments for both HCl and HBr photodissociation.

In contrast to the $a_0^1(\perp)$ parameter, calculating an inferred value of the $\operatorname{Re}[a_1^1(\parallel,\perp)]$ parameter is more complicated. The $\operatorname{Re}[a_1^1(\parallel,\perp)]$ parameter depends on phase coher-

TABLE II. A summary of previously published experimental and *ab initio* vales of polarization parameters $a_0^1(\perp)$ and $\operatorname{Re}[a_1^1(\parallel,\perp)]$ for the halogen-atom photofragments from the photodissociation of HCl and HBr (Refs. 10, 13, 43, and 44). Note that the sign of the parameter $\operatorname{Re}[a_1^1(\parallel,\perp)]$ used here has been corrected from Refs. 10 and 13. The uncertainties represent 2σ of the values.

		HCl photodissociation Expt.	HCl photodissociation *Ab initio*	HBr photodissociation Expt.	HBr photodissociation *Ab initio*
$a_0^1(\perp)$	$Y(^2P_{3/2})$	$+0.39\pm0.08$	$+0.413$	$+0.30\pm0.07$	$+0.35$
	$Y^*(^2P_{1/2})$	$+0.60\pm0.10$	$+0.577$	$+0.55\pm0.16$	$+0.577$
$\operatorname{Re}[a_1^1(\parallel,\perp)]$	$Y(^2P_{3/2})$	$+0.06\pm0.10$	-0.044	-0.09 ± 0.08	$+0.031$
	$Y^*(^2P_{1/2})$	$+0.32\pm0.10$	$+0.10$	-0.46 ± 0.16	$+0.36$

(a)

Probe wavelength (nm)

HCl

LL

RL

(b)

$P_X \sin \theta$

pump

$P_Z \cos \theta$ probe

(pump L)

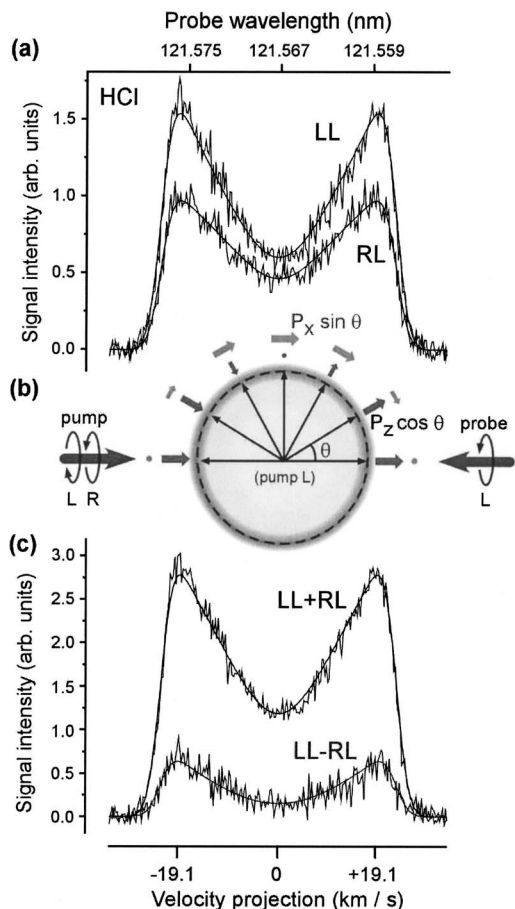L R

L

(c)

LL+RL

LL−RL

Velocity projection (km / s)

FIG. 7. SPH detection from HCl photodissociation at 193 nm. (a) Experimental fluorescence signals I_{LL} and I_{RL}. (b) The spherical velocity distribution of the SPH, showing the SPH polarization as a function of angle with respect to the laser propagation axis, showing $P_Z \cos \theta$, the polarization component parallel to the atom recoil direction **v**, and $P_X \sin \theta$, the polarization component perpendicular to **v**. Both P_Z and P_X have positive projections along $+Z^{\text{lab}}$. The one-dimensional projection of this distribution gives the experimental signals. (c) The sum $I_{LL}+I_{RL}$ and difference $I_{LL}-I_{RL}$ of traces in (a). The sum trace depends only on the velocity distribution of the H atoms, and the difference trace is proportional to the SPH polarization [see Eqs. (7a) and (7b)].

ence between parallel ($\parallel$) and perpendicular ($\perp$) states. For the ground-state Cl atoms this involves more than one pair of interfering states, namely, $A1$, $X0$ and $a1$, $X0$. In order to obtain a value, we require both $\text{Re}[a_1^1(\parallel, \perp)]$ and $\text{Re}[a_1^2(\parallel, \perp)]$ for Cl to obtain the two phases: The details are given in the Appendix. We find that the present experimental results are in reasonably good agreement with the values inferred from the Cl/Cl* and Br/Br* atoms. However, the *ab initio* results do not agree very well with the experiments, and we see that this could have been expected from the halogen-atom results. The exact origin of the discrepancy at present is not understood. It is evident that, so far, the calculations tend to overestimate the contribution from perpendicular excitations, e.g., it is found that for Cl* atoms $\beta=-0.87$ (experiment), whereas $\beta=-0.989$ (theory).[44] Recent calculations by Truhlar *et al.*[50] specifically looking at the spin-orbit coupling in the HBr system, suggest an increased contribution from excitation to the $a0$ state. It is well recognized that the polarization parameters $\text{Re}[a_1^k(\parallel, \perp)]$ that depend on coherence are very sensitive to the shapes of the
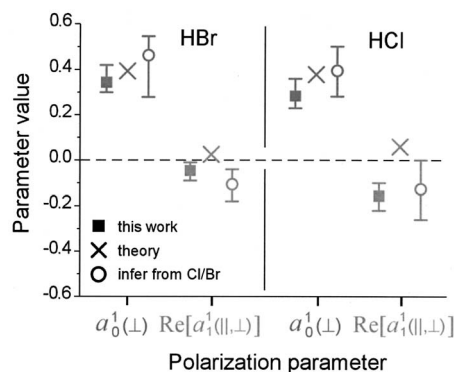
FIG. 8. Analysis of the experimental profiles, using Eq. (7), yields values of $a_0^1(\perp)$ and $\text{Re}[a_1^1(\parallel, \perp)]$ for the H-atom photofragments from the photodissociation of HCl, shown here along with the results from the photodissociation of HBr (solid squares), from Ref. 41. These values are compared with *ab initio* calculated values (crosses), from Refs. 43 and 44, and values inferred from the Br and Cl cofragment polarizations (open circles), from Refs. 10 and 13. The lower error bars represent 2σ of the fitted values, determined by a Monte Carlo sampling procedure (Ref. 49). The upper error bars also include the uncertainty in the degree of circular polarization of the 121.6 nm light.

potential energy curves.[51] In the present case, given the breadth of evidence for significant nonadiabatic dynamics, there may be significant additional phase (i.e., dynamical phase) terms that have not thus far been included in the calculations. It is clear that HCl and HBr continue to set the high bar for further investigations of photodissociation dynamics.

The $a_0^1(\perp)$ parameter can be related to the spin polarization of the H atoms along the recoil direction P_Z by $P_Z = \sqrt{3}a_0^1(\perp)$. The $\text{Re}[a_1^1(\parallel, \perp)]$ parameter can be related to the spin polarization of the H atoms along the X axis in the molecular frame, perpendicular to the recoil direction but in the plane of the photolysis polarization, by $P_X = -\sqrt{3/2}\,\text{Re}[a_1^1(\parallel, \perp)]/(1+\beta/4)$. Using these relations, we find that the spin polarizations of the H atoms are given by $P_Z = 0.48^{+0.14}_{-0.09}$ and $P_X = 0.25 \pm 0.10$ for the case of HCl photodissociation and $P_Z = 0.59^{+0.14}_{-0.07}$ and $P_X = 0.07 \pm 0.06$ for the case of HBr photodissociation (all errors 2σ).

We consider briefly the effects of temperature of the sample on the coherent polarization moments of the product H atoms. Calculations of Lambert *et al.*[52] suggest that parent rotation (J_{HCl}) has almost no effect on the product branching into Cl and Cl* product channels, and therefore we do not expect the H-atom polarization to be significantly affected by effects of Coriolis coupling. So far there have been no calculations of the effects of J_{HCl} on the spatial distribution (β), which would indicate a shift in the proportion of excitations to the parallel and perpendicular states. At the temperatures of the beam experiments (15 K), more than 70% of the parent molecule population is in $J_{\text{HCl}}=0$, and for the present experiments at room temperature (295 K) the population peaks at $J_{\text{HCl}}=3$ with more than 90% of the population in levels, $J_{\text{HCl}} \leq 6$. From a mechanical point of view, the axial rotation of the molecule is very small compared to the high velocity of the H atoms (19.1 km s^{-1}), and therefore we expect the axial recoil approximation to be entirely valid even at $J_{\text{HCl}}=6$.[53] We have looked at the effects of an additional

TABLE III. Analysis of the experimental profiles, using Eq. (7), yields values of $a_0^1(\perp)$ and $\mathrm{Re}[a_1^1(\|, \perp)]$ for the H-atom photofragments from the photodissociation of HCl, shown here along with the results from the photodissociation of HBr, from Ref. 41. These values are compared with *ab initio* calculated values, from Refs. 43 and 44, and values inferred from the Br/Br* and Cl/Cl* cofragment polarizations, from Refs. 10 and 13. The uncertainties represent 2σ of the values. For the present work, the upper error bars also include uncertainty in the degree of circular polarization of the 121.6 nm light (see text for details).

	HCl photodissociation			HBr photodissociation		
	Expt.	*ab initio*	Infer from Cl/Cl*	Expt.	*ab initio*	Infer from Br/Br*
$a_0^1(\perp)$	$0.28^{+0.08}_{-0.05}$	0.38	0.39 ± 0.11	$0.34^{+0.08}_{-0.04}$	0.39	0.46 ± 0.18
$\mathrm{Re}[a_1^1(\|, \perp)]$	-0.16 ± 0.06	0.059	-0.13 ± 0.13	-0.05 ± 0.04	0.025	-0.11 ± 0.07

centrifugal potential $E_{\mathrm{cent}} = \hbar^2 J(J+1)/2\mu r^2$ (where r is the HCl internuclear distance) on the asymptotic phase difference. We carried out semiclassical calculations of the phase difference $\cos \Delta \phi_{ta}$ using the $t1$ and $a0$ electronic potential energy curves of Lambert *et al.* (for H atoms paired with Cl*).[43,54] The semiclassical methods used have been detailed elsewhere.[51] We find that, compared to $J_{\mathrm{HCl}}=0$, the value of $\cos \Delta \phi_{ta}$ has changed by only 2% for $J_{\mathrm{HCl}}=3$ and by 8% for $J_{\mathrm{HCl}}=6$; these changes are well within the uncertainties of the present experiment. We emphasize that the present experiments reported here show that the photodissociation of room-temperature samples of HBr and HCl at 193 nm yield highly spin-polarized hydrogen atoms. The lack of the need of supersonic cooling increases the applicability of HCl or HBr photodissociation as versatile SPH sources and allows extremely high molecular and pulsed SPH densities to be achieved.

In our experiments, the detection of the complete speed distribution of the H atoms is achieved only when the photolysis and probe laser beams are overlapped temporally. Otherwise, the speed of the H atoms is large enough that at even fairly small pump-probe time delays, the H atoms with speeds that are not nearly parallel to the laser propagation direction fly out of the probe volume and are not detected. This effect, known as VADS, was discussed in the Introduction as a method of photofragment velocity selection. An example of this is shown in Fig. 9. HCl molecules are photodissociated with a photolysis-probe delay of about 100 ns; only two sharp peaks are visible, which correspond to H atoms with velocities that are parallel and antiparallel to the probe propagation direction.

The method of detection of the spin polarization of H atoms shown here uses fluorescence, whereas, in recent years, for most studies of molecular photodissociation, the photofragments are detected using some form of laser ionization. Ionization and fluorescence are complementary detection techniques and have different realms of application. One reason that we used fluorescence is that we could not find a one-color scheme of laser ionization that can detect the H-atom spin polarization with maximum (or any) sensitivity, without needing to resolve the fine structure of H atoms.[35] Two other fluorescence schemes, in addition to the one that is demonstrated here, were proposed.[42] One of these schemes, the two-photon $2s \leftarrow \leftarrow 1s$ transition at 243 nm, followed by excitation of the $4p \leftarrow 2s$ transition at 486 nm, and the subsequent detection of fluorescence at 486 nm was attempted by our group. No spin polarization was detected within the signal-to-noise ratio of the experiment, and the (I_{YY}/I_{XY}) ratio was measured to be approximately 1 for HCl pressures of about 1 mbar. We did not conclusively determine the reason for the failure of the scheme (such as whether the depolarization cross section of the $4p$ state is much larger than the $2p$ state or whether the laser overlap of the intense 243 nm light causes any problems with the fluorescence of the $4p$ state) but concluded that the scheme presented here seems to be more robust.

A two- or three-color ionization scheme, which detects the H-atom spin polarization with maximum sensitivity without needing fine-structure resolution, seems feasible. One such scheme, shown in Fig. 10, is the excitation with linearly polarized 121.6 nm light to the $2p$ state, followed by two-photon excitation with circularly polarized 1313 nm light to the $3p$ state, followed by ionization. The ionization step can be achieved either with two photons of 1313 nm or by some other color which ionizes the $3p$ state with one photon, but requires two photons to ionize the $2p$ state so that the $3p$ state is ionized much more efficiently than the $2p$ state; this condition is satisfied for wavelengths between about 364.7 and 820.6 nm (for example, the residual 532 nm light from a YAG laser can be used). Note, however, that the polarization axis of the linearly polarized 121.6 nm beam must be parallel to the propagation direction of the 1313 nm light beam, achieved only by crossing the two probe laser beams.
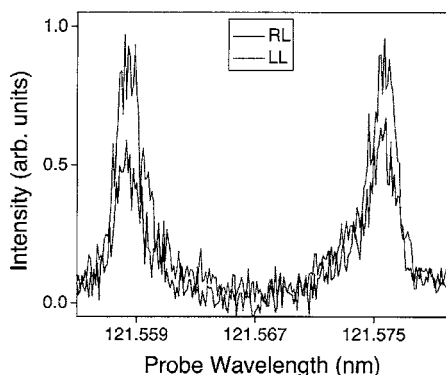

FIG. 9. Spin-polarized H atoms from the photodissociation of HCl at a pump-probe delay of 100 ns. Only the H atoms with velocities that are nearly parallel or antiparallel to the probe laser propagation direction remain in the probe volume and are detected.
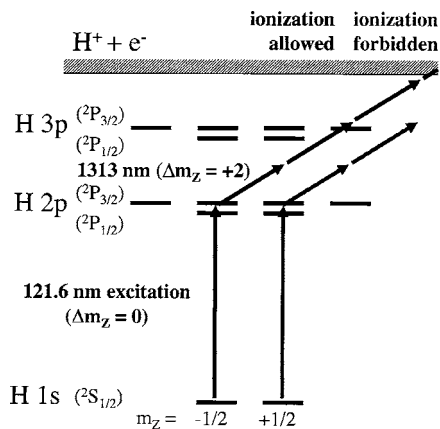
FIG. 10. Scheme for the spin-state specific ionization of hydrogen atoms. Linearly polarized excitation of the $2p \leftarrow 1s$ transition is followed by two-photon circularly polarized excitation of the $3p \leftarrow 2p$ transition, followed by ionization. Resolution of the fine structure is not required.

ACKNOWLEDGMENTS

APPENDIX: INFERRING Re[$a_1^1(\|, \perp)$] FROM HALOGEN ATOMS

The Re[$a_1^1(\|, \perp)$] for the H atom can be inferred from measured polarization parameters for the cofragment halogen atoms Y and Y^*. According to the branching to Y and Y^* channels we need to make a weighted sum of inferred Re[$a_1^1(\|, \perp)$] for H atoms partnered with Y and Y^*, respectively:

$$\text{Re}[a_1^1(\|, \perp)](H) = f\,\text{Re}[a_1^1(\|, \perp)](H; Y)$$
$$+ (1 - f)\text{Re}[a_1^1(\|, \perp)](H; Y^*), \quad (A1)$$

where the branching fractions are $f = 0.59$ for HCl and $f = 0.86$ for HBr. The polarization parameters for H partnered with Y and Y^* atoms can be written in terms of scattering phases between the dissociating states[2,55]

$$\text{Re}[a_1^1(\|, \perp)](H; Y^*) = -\sqrt{6}\left(\frac{r_{t1}r_{a0}}{r_{a0}^2 + 2r_{r1}^2}\right)\cos\Delta\varphi_{ta}, \quad (A2)$$

$$\text{Re}[a_1^1(\|, \perp)](H; Y) = \sqrt{6}\left(\frac{r_{a1}r_{X0}}{r_{X0}^2 + 2r_{A1}^2 + 2r_{a1}^2}\right)\cos\Delta\varphi_{aX},$$
$$(A3)$$

where $\Delta\phi_{10} = \phi_{\Omega=1} - \phi_{\Omega=0}$ are the phase differences and r_Ω are the scattering amplitudes into different product channels of the dissociation. For the Y^* channel there is coherence

only between $t1$ and $a0$ states; both H-atom and halogen-atom fragments have $J = 1/2$, and we obtain

$$\text{Re}[a_1^1(\|, \perp)](H; Y^*) = \text{Re}[a_1^1(\|, \perp)](Y^*). \quad (A4)$$

The previously published orientation parameters Re[$a_1^1(\|, \perp)$](Y^*) for Cl* and Br* are given in Table II. For the Y channel, we find that there are coherences involving the pairs $(A1, X0)$ and $(a1, X0)$, and the Y-atom parameter can be written as

$$\text{Re}[a_1^1(\|, \perp)](Y) = \frac{12}{\sqrt{40}}\left(\frac{r_{A1}r_{X0}}{r_{X0}^2 + 2r_{A1}^2 + 2r_{a1}^2}\right)\cos\Delta\varphi_{AX}$$
$$- \frac{12}{\sqrt{30}}\left(\frac{r_{a1}r_{X0}}{r_{X0}^2 + 2r_{A1}^2 + 2r_{a1}^2}\right)\cos\Delta\varphi_{aX}.$$
$$(A5)$$

However, the H-atom parameter Re[$a_1^1(\|, \perp)$](H; Y) only depends on $\cos\Delta\phi_{aX}$, so we require an additional polarization parameter for Y atoms to infer the value for H atoms partnered by Y. We use

$$\text{Re}[a_1^2(\|, \perp)](Y) = \frac{12\sqrt{2}}{5}\left(\frac{r_{A1}r_{X0}}{r_{X0}^2 + 2r_{A1}^2 + 2r_{a1}^2}\right)\cos\Delta\varphi_{AX}.$$
$$(A6)$$

By combining Eqs. (A3), (A5), and (A6) we finally obtain

$$\text{Re}[a_1^1(\|, \perp)](H; Y) = \frac{5}{8}\text{Re}[a_1^2(\|, \perp)](Y)$$
$$- \frac{\sqrt{5}}{2}\text{Re}[a_1^1(\|, \perp)](Y). \quad (A7)$$

Values obtained from Eqs. (A4) and (A7) can be combined to give the final inferred value Re[$a_1^1(\|, \perp)$](H) for H atoms, using Eq. (A1). The previously published orientation parameters Re[$a_1^1(\|, \perp)$](Y) for Cl and Br are given in Table II. The alignment parameters Re[$a_1^2(\|, \perp)$] for Cl and Br atoms were obtained from the previously published work of Rakitzis *et al.*[9] In that work, the parameter Re[$a_1^2(\|, \perp)$] was taken to be identically zero to a first approximation because the dissociation is very nearly all perpendicular in character (>96%). The more recent measurements of Re[$a_1^1(\|, \perp)$](Y) for Br and Cl, however, suggest that the coherences involved are non-negligible. We have reanalyzed the alignment data from Rakitzis *et al.* to obtain Re[$a_1^2(\|, \perp)$](Cl) = 0.12 ± 0.12 and Re[$a_1^2(\|, \perp)$](Br) = -0.24 ± 0.24 (errors 2σ), with the other parameters $a_0^2(\perp)$ and $a_2^2(\perp)$ being largely unchanged within their published uncertainties. The final values for Re[$a_1^1(\|, \perp)$](H) inferred from the halogen polarization parameters are shown in Fig. 8 and are given in Table III.

[1] A. G. Smolin, O. S. Vasyutinskii, and A. J. Orr-Ewing, Mol. Phys. **105**, 885 (2007).
[2] G. G. Balint-Kurti, A. J. Orr-Ewing, J. A. Beswick, A. Brown, and O. S. Vasyutinskii, J. Chem. Phys. **116**, 10760 (2002).
[3] A. P. Clark, M. Brouard, F. Quadrini, and C. Vallance, Phys. Chem. Chem. Phys. **8**, 5591 (2006).
[4] M. L. Costen and G. E. Hall, Phys. Chem. Chem. Phys. **9**, 272 (2007).
[5] S. K. Lee, R. Silva, S. Thamanna, O. S. Vasyutinskii, and A. G. Suits, J. Chem. Phys. **125**, 144318 (2006).
[6] T. P. Rakitzis, S. A. Kandel, A. J. Alexander, Z. H. Kim, and R. N. Zare, Science **281**, 1346 (1998).
[7] L. D. A. Siebbeles, M. Glass-Maujean, O. S. Vasyutinskii, J. A. Beswick,

and O. Roncero, J. Chem. Phys. **100**, 3610 (1994).

[8] A. S. Bracker, E. R. Wouters, A. G. Suits, and O. S. Vasyutinskii, J. Chem. Phys. **110**, 6749 (1999).

[9] T. P. Rakitzis, P. C. Samartzis, R. L. Toomes, L. Tsigaridas, M. Coriou, D. Chestakov, A. T. J. B. Eppink, D. H. Parker, and T. N. Kitsopoulos, Chem. Phys. Lett. **364**, 115 (2002).

[10] T. P. Rakitzis, P. C. Samartzis, R. L. Toomes, T. N. Kitsopoulos, A. Brown, G. G. Balint-Kurti, O. S. Vasyutinskii, and J. A. Beswick, Science **300**, 1936 (2003).

[11] T. P. Rakitzis and T. N. Kitsopoulos, J. Chem. Phys. **116**, 9228 (2002).

[12] A. G. Smolin, O. S. Vasyutinskii, O. P. J. Vieuxmaire, M. N. R. Ashfold, G. G. Balint-Kurti, and A. J. Orr-Ewing, J. Chem. Phys. **124**, 094305 (2006).

[13] T. P. Rakitzis, P. C. Samartzis, R. L. Toomes, and T. N. Kitsopoulos, J. Chem. Phys. **121**, 7222 (2004).

[14] A. T. J. B. Eppink, D. H. Parker, M. H. M. Janssen, B. Buijsse, and W. J. van der Zande, J. Chem. Phys. **108**, 1305 (1998).

[15] M. Ahmed, D. S. Peterka, A. S. Bracker, O. S. Vasyutinskii, and A. G. Suits, J. Chem. Phys. **110**, 4115 (1999).

[16] S. J. Horrocks, G. A. D. Ritchie, and T. R. Sharples, J. Chem. Phys. **127**, 114308 (2007).

[17] M. Brouard, R. Cireasa, A. P. Clark, F. Quadrini, and C. Vallance, Phys. Chem. Chem. Phys. **8**, 5549 (2006).

[18] A. M. Coroiu, D. H. Parker, G. C. Groenenboom, J. Barr, I. T. Novalbos, and B. J. Whitaker, Eur. Phys. J. D **151**, 206 (2006).

[19] M. Brouard, R. Cireasa, A. P. Clark, T. J. Preston, and C. Vallance, J. Chem. Phys. **124**, 064309 (2006).

[20] S. K. Lee, D. Townsend, O. S. Vasyutinskii, and A. G. Suits, Phys. Chem. Chem. Phys. **7**, 1650 (2005).

[21] Y. Mo, H. Katayanagi, M. C. Heaven, and T. Suzuki, Phys. Rev. Lett. **77**, 830 (1996).

[22] T. P. Rakitzis, P. C. Samartzis, and T. N. Kitsopoulos, Phys. Rev. Lett. **87**, 123001 (2001).

[23] D. Townsend, S. K. Lee, and A. G. Suits, Chem. Phys. **301**, 197 (2004).

[24] M. Brouard, A. V. Green, F. Quadrini, and C. Vallance, J. Chem. Phys. **127**, 084304 (2007).

[25] M. Brouard, F. Quadrini, and C. Vallance, J. Chem. Phys. **127**, 084305 (2007).

[26] A. J. van den Brom, T. P. Rakitzis, and M. H. M. Janssen, J. Chem. Phys. **123**, 164313 (2005).

[27] R. J. van Brunt and R. N. Zare, J. Chem. Phys. **48**, 4304 (1968).

[28] O. S. Vasyutinskii, Sov. Phys. JETP **54**, 855 (1981).

[29] M. Glass-Maujean, R. Kneip, E. Flemming, and H. Schmoranzer, J. Phys. B **38**, 2871 (2005).

[30] M. Glass-Maujean and H. Schmoranzer, J. Phys. B **38**, 1093 (2005).

[31] M. Glass-Maujean, S. Klumpp, L. Werner, A. Ehresmann, and H. Schmoranzer, J. Phys. B **37**, 2677 (2004).

[32] M. Glass-Maujean, S. Lauer, H. Liebel, and H. Schmoranzer, J. Phys. B **34**, 5121 (2001).

[33] E. Flemming, O. Wilhelmi, H. Schmoranzer, and M. Glass-Maujean, J. Chem. Phys. **103**, 4090 (1995).

[34] J. D. Bozek, J. E. Furst, T. J. Gay, H. Gould, A. L. D. Kilcoyne, J. R. Machacek, F. Martín, K. W. McLaughlin, and J. L. Sanz-Vicario, J. Phys. B **39**, 4871 (2006); **41**, 039801 (2008).

[35] H. Rottke and H. Zacharias, Phys. Rev. A **33**, 736 (1986).

[36] O. J. Luiten, H. G. C. Werij, I. D. Setija, M. W. Reynolds, T. W. Hijmans, and J. T. M. Walraven, Phys. Rev. Lett. **70**, 544 (1993).

[37] M. Johnson, L. Pringle, X. Zhang, K. T. Lorenz, and B. Koplitz, J. Phys. Chem. A **107**, 8134 (2003).

[38] K. A. Cowen, K. T. Lorenz, Y.-F. Yen, M. F. Herman, and B. Koplitz, J. Chem. Phys. **103**, 5864 (1995).

[39] K. T. Lorenz, K. A. Cowen, P. F. Fleming, M. G. Mathews, M. F. Herman, and B. Koplitz, Chem. Phys. Lett. **261**, 145 (1996).

[40] X. Zhang, M. Johnson, K. T. Lorenz, K. A. Cowen, and B. Koplitz, J. Phys. Chem. A **104**, 10511 (2000).

[41] D. Sofikitis, L. Rubio-Lago, A. J. Alexander, and T. P. Rakitzis, Europhys. Lett. **81**, 69002 (2008).

[42] T. P. Rakitzis, ChemPhysChem **5**, 1489 (2004).

[43] A. G. Smolin, O. S. Vasyutinskii, G. G. Balint-Kurti, and A. Brown, J. Phys. Chem. A **110**, 5371 (2006).

[44] A. Brown, G. G. Balint-Kurti, and O. S. Vasyutinskii, J. Phys. Chem. A **108**, 7790 (2004).

[45] R. N. Zare, *Angular Momentum: Understanding Spatial Aspects in Chemistry and Physics* (Wiley-Interscience, New York, 1988).

[46] A. J. Alexander, Z. H. Kim, S. A. Kandel, R. N. Zare, T. P. Rakitzis, Y. Asano, and S. Yabushita, J. Chem. Phys. **113**, 9022 (2000).

[47] A. J. Alexander, J. Chem. Phys. **123**, 194312 (2005).

[48] H. Winter and H. W. Ortjohann, Rev. Sci. Instrum. **58**, 359 (1987).

[49] A. J. Alexander, D. A. Blunt, M. Brouard, J. P. Simons, F. J. Aoiz, L. Banares, Y. Fujimura, and M. Tsubouchi, Faraday Discuss. **108**, 375 (1997).

[50] R. Valero, D. G. Truhlar, and A. W. Jasper, J. Phys. Chem. A **112**, 5756 (2008).

[51] A. J. Alexander and T. P. Rakitzis, Mol. Phys. **103**, 1665 (2005).

[52] H. M. Lambert, P. J. Dagdigian, and M. H. Alexander, J. Chem. Phys. **108**, 4460 (1998).

[53] E. Wrede, E. R. Wouters, M. Beckert, R. N. Dixon, and M. N. R. Ashfold, J. Chem. Phys. **116**, 6064 (2008).

[54] M. H. Alexander, B. Pouilly, and T. Duhoo, J. Chem. Phys. **99**, 1752 (1993).

[55] A. J. Alexander, Phys. Chem. Chem. Phys. **7**, 3693 (2005).